

Chapter 15

Heat Regenerators: Direct-Contact Heat Storing Exchangers Using a Batch of Solids

“The theories of the regenerator are among the most difficult and involved that are encountered in engineering.”

M. Jacob

Because solids, on a volume basis, have a very large heat capacity compared to gases, they can effectively be used as an intermediary in the transfer of heat from one gas to another. This requires a two-step operation. In the first step hot gas gives up its heat to cold solids. The solids heat up, and then in the second step, the solids release this heat to a second cold gas. For continuous operations regenerators are used in pairs, as shown in Fig. 15.1.

This type of storage exchanger is used primarily when heat has to be exchanged between enormous amounts of gas, as in the steel and other metallurgical industries, or when the gases are dirty and dust laden and liable to plug up a recuperator, as is the case with flue gases in coal-burning electric power stations, or when one of the gases is too hot or reactive for the materials of construction of a recuperator, as is the case with gases from glassmaking furnaces.

Regenerators can also be designed for continuous operations as shown in Fig. 15.2.

In turn, let us take up the two major classes of regenerators: first, the fixed solid devices (the packed bed, the rotating wheel, the monolith unit) and then the well-mixed solid devices (the single-stage and the multistage fluidized bed).

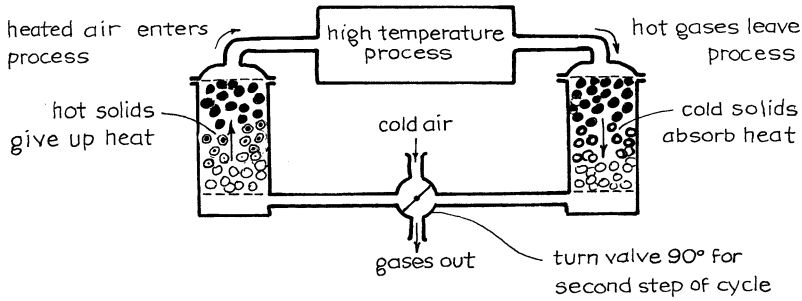


Fig. 15.1 A pair of cyclic regenerators for recovering heat from waste gas

15.1 Packed Bed Regenerators: Preliminary

15.1.1 Spreading of a Temperature Front

These units are usually packed with large solids—bricks, rocks—so that the pressure drop for gas flow does not become excessive and so that fine solids suspended and entrained by the gas do not plug up the unit.

When hot gas enters an initially cold bed of solids, a hot temperature front of gas moves down the bed trailed by a hot front of solids, as shown in Fig. 15.3. Three phenomena lead to the spreading of these hot fronts:

- Deviation from plug flow of gas in the packed bed—some fluid moving faster, some moving slower. This behavior is characterized by the axial dispersion coefficient for the gas D , a sort of diffusion coefficient.
- Film resistance to heat transfer between gas and solid. Since the particles are large, the interfacial area and the heat transfer coefficient ha can be very much lower than for beds of fine solids. The term ha characterizes this resistance.
- Resistance to heat flow into the particles. With large solids such as bricks and rocks, the characteristic time for the heating of the particles can be large. The thermal diffusivity of the solids $k_s/\rho_s C_s$ characterizes this resistance.

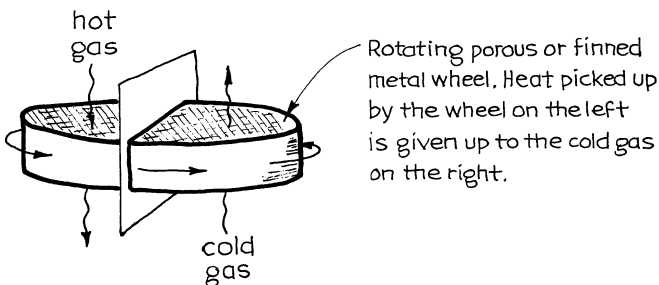


Fig. 15.2 Continuously operating rotating-wheel regenerator

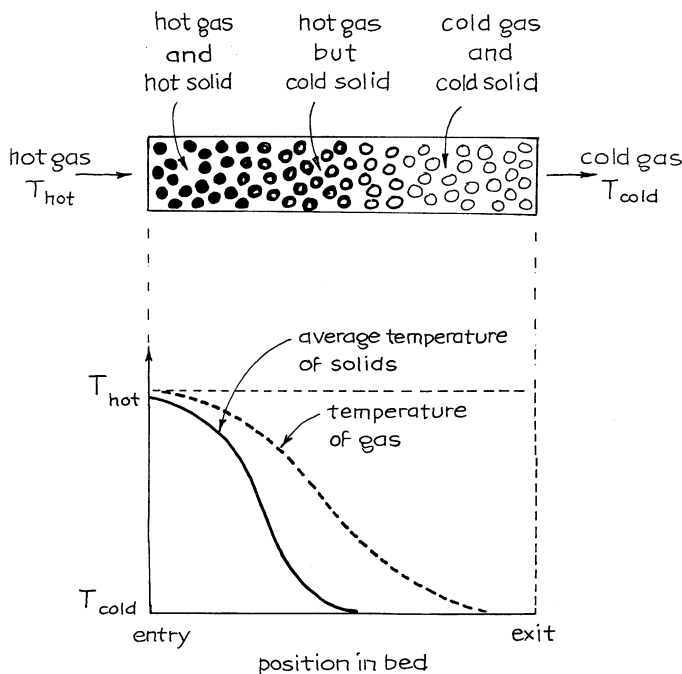


Fig. 15.3 Advancing temperature front in gas and in solid in a packed bed regenerator

15.1.2 Models for the Temperature Spread

We have three levels of analysis for fixed bed regenerators, as shown in Fig. 15.4:

1. The *flat front approximation* of Fig. 15.4a is the simplest model. It assumes ideal plug flow of gas and immediate equalizing of gas and solid temperature. This is a crude approximation, but still useful for baseline estimates of behavior.
2. The *dispersion approach* of Fig. 15.4b describes each of the three spreading factors by a diffusion-like phenomenon. This leads to a symmetrical S-shaped temperature–distance curve for solids characterized by its variance σ^2 . Assuming independence of the three spreading phenomena, we can add the variances to give

$$\sigma_{\text{overall}}^2 = \underbrace{\sigma_{\text{gas}}^2}_{\text{dispersion}} + \underbrace{\sigma_{\text{film}}^2}_{\text{resistance}} + \underbrace{\sigma_{\text{particle}}^2}_{\text{conduction}} \quad (15.1)$$

This approach should reasonably approximate the real temperature distribution in a not-too-short regenerator.

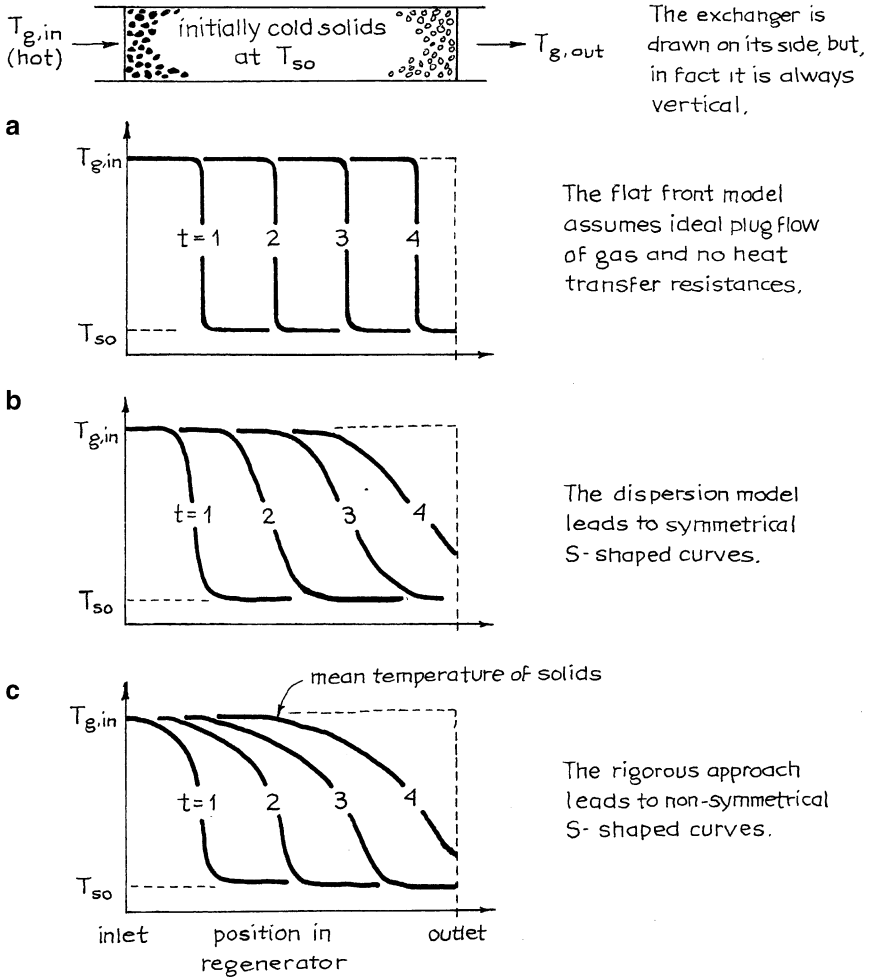


Fig. 15.4 Temperature of solids in a packed bed regenerator according to different models from the simplest to the most complicated

3. The *rigorous analysis* which accounts properly for all three spreading phenomena should yield unsymmetrical S-shaped curves sketched in Fig. 15.4c. This analysis is extremely difficult and has not as yet been done. The many approaches and partial solutions to this problem are presented and discussed by Hausen (1983) and Jakob (1957). Other related references are presented by McAdams (1954) and Kern (1950).

We will take up the flat front and dispersion approaches in analyzing both single-pass and periodic operations of heat regenerators. We do not attempt the rigorous approach.

15.1.3 Measure of Thermal Recovery Efficiency

Suppose hot gas at $T_{h,in}$ enters a cold regenerator at T_c for a length of time t . We define the *efficiency of heat capture by solids* or the *efficiency of heat removal from the gas* for this period as

$$\begin{aligned} \eta_h &= \left(\frac{\text{heat taken up by cold solids}}{\text{maximum possible take up}} \right) = \left(\frac{\text{heat lost by hot gas}}{\text{maximum possible heat loss in time } t} \right) \\ &= \left(\frac{\overline{\Delta T}_h}{\Delta T_{\max}} \right)_{\text{of gas}} = \left(\frac{T_{h,in} - \overline{T}_{h,out}}{T_{h,in} - T_c} \right)_{\text{of gas}} \end{aligned} \quad (15.2)$$

Similarly, for cold gas at $T_{c,in}$ entering a hot regenerator T_h for a time period t ,

$$\begin{aligned} \eta_h &= \left(\frac{\text{heat lost by solids}}{\text{maximum possible}} \right) = \left(\frac{\text{heat gained by cold gas}}{\text{maximum possible heat gain in time } t} \right) \\ &= \left(\frac{\overline{\Delta T}_c}{\Delta T_{\max}} \right)_{\text{gas}} = \left(\frac{\overline{T}_{c,out} - T_{c,in}}{T_h - T_{c,in}} \right)_{\text{gas}} \end{aligned} \quad (15.3)$$

Let us relate these efficiencies. For this consider hot fluid entering an initially cold regenerator. Making a heat balance at time t gives

$$\begin{aligned} \text{Fraction of solids heated} &= \left(\frac{\text{heat introduced by gas in time } t}{\text{heat needed to heat up all the solids}} \right) \\ &= \frac{\dot{m}_h C_h (T_{h,in} - T_c) t}{W_s C_s (T_{h,in} - T_c)} = \frac{\dot{m}_h C_h t}{W_s C_s} \end{aligned} \quad (15.4)$$

The characteristic time needed to heat all the solids is then

$$\hat{t}_h = \frac{W_s C_s}{\dot{m}_h C_h} = \frac{\rho_s (1 - \epsilon) C_s}{G_h C_h} \cdot L \quad (15.5)$$

Similarly, for the cooling of initially hot solids we have

$$\hat{t}_c = \frac{W_s C_s}{\dot{m}_c C_c} = \frac{\rho_s (1 - \epsilon) C_s}{G_c C_c} \cdot L \tag{15.6}$$

When $\hat{t}_h = \hat{t}_c$ we have what is called *symmetric operations*. For unequal flow rates of hot and cold gases, the characteristic heating and cooling times will differ, or $\hat{t}_h \neq \hat{t}_c$, and we have *unsymmetric operations*.

We will show that symmetric operations are simpler to analyze, always give a higher heat exchange efficiency, and should therefore always be used in practice. We treat this situation.

15.1.4 Periodic Cocurrent and Countercurrent Operations

Periodic operations can be run in two ways. In cocurrent operations the cold fluid and the hot fluid enter one after the other at the same end of the regenerator. In countercurrent operations the hot fluid enters at one end, the cold fluid at the other end of the regenerator. These two modes are shown in Fig. 15.5.

It is not obvious which of these contacting patterns is better. The simple flat front model says that both can be equally good. However, as we will show, the dispersion model predicts that countercurrent operations have a higher efficiency. We will analyze both modes of operations.

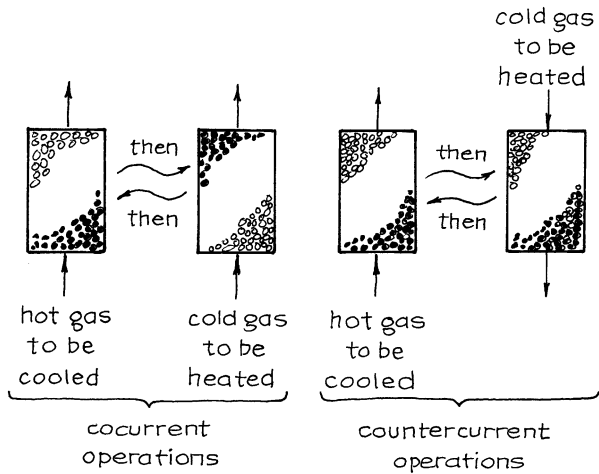


Fig. 15.5 Switching pattern for periodic cocurrent and periodic countercurrent operations of a packed bed regenerator

15.2 Packed Bed Regenerators: Flat Front Model

15.2.1 Cocurrent Operations with $\hat{t}_h = \hat{t}_c = \hat{t}$

Let hot and cold fluid flow through the two side-by-side regenerators at the same rate, and by this we mean that the temperature fronts move through the regenerators at the same speed. In symbols this says that $\dot{m}_h C_h = \dot{m}_c C_c$ or that $\hat{t}_h = \hat{t}_c$. Let us call this time \hat{t} .

If the switching time is chosen to be $\hat{t}_h = \hat{t}_c$, then the heat given up by the hot gas is just enough to heat the regenerator. This represents the most efficient heat interchange scheme, or

$$\eta_h = \eta_c = 100 \% \quad \text{for } t_{sw} = \hat{t} \tag{15.7}$$

If the switching time is shorter than $\hat{t}_h = \hat{t}_c$, then

$$\eta_h = \eta_c = 2 - \frac{\hat{t}}{t_{sw}} \quad \text{for } t_{sw} = \text{between } \frac{2}{3}\hat{t} \text{ and } \hat{t} \tag{15.8}$$

If the switching time is longer than $\hat{t}_h = \hat{t}_c$, then

$$\eta_h = \eta_c = \frac{\hat{t}}{t_{sw}} \quad \text{for } t_{sw} > \hat{t} \tag{15.9}$$

Figure 15.6 shows one pair of regenerators for the two undesirable situations above. These results show that one should always use cocurrent switching times equal to $\hat{t}_h = \hat{t}_c$. Unsymmetric operations can never give 100 % exchanger efficiency and should be avoided.

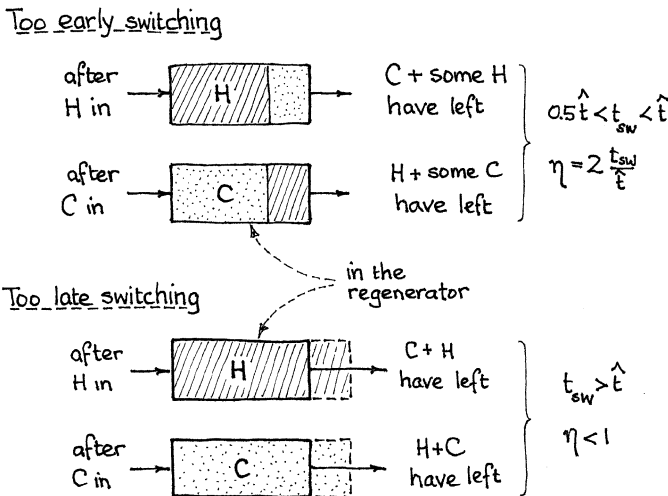


Fig. 15.6 Cocurrent pair of heat regenerators

15.2.2 Countercurrent Operations with $\hat{t}_h = \hat{t}_c = \hat{t}$

By referring to sketches of Fig. 15.7, we see that if $t_{sw} \leq \hat{t}$, then the temperature front remains in the regenerator, moving from right to left, but never spilling out of either end. For this situation

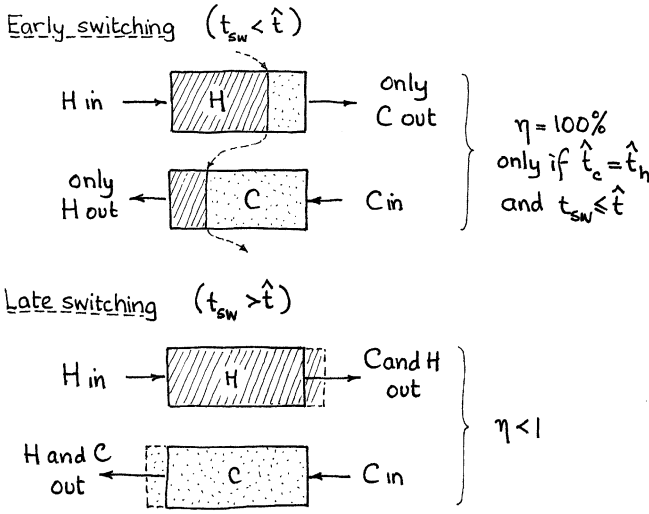


Fig. 15.7 Countercurrent pair of heat regenerators

$$\eta_h = \eta_c = 100 \% \quad \text{for } t_{sw} \leq \hat{t} \tag{15.10}$$

If the switching time is delayed, $t_{sw} > \hat{t}$, the front will spill over the regenerator exits, hot and cold fluids will mix, and so the exchanger efficiency will be lowered to

$$\eta_h = \eta_c = \frac{\hat{t}}{t_{sw}} \quad \text{for } t_{sw} \geq \hat{t} \tag{15.11}$$

Finally, even if $t_{sw} < \hat{t}_h$ and \hat{t}_c , if $\hat{t}_h \neq \hat{t}_c$, then the heat front will move back and forth but will eventually drift to one end or the other of the regenerator and will spill from the unit, thereby lowering the exchanger efficiency.

15.2.3 Comments on the Flat Front Model

This model shows that countercurrent flow is more flexible than cocurrent flow in that it can give 100 % efficiency for any $t_{sw} < \hat{t}$. However, it also tells that you must use $\hat{t}_h = \hat{t}_c$; otherwise, your efficiency drops no matter what switching time is used.

Finally, this model is a useful first approximation. In the more realistic dispersion model, which we treat next, we will see that the predicted flat front efficiencies are higher than would be found in practice.

15.3 Packed Bed Regenerators: Dispersion Model

Consider in turn:

- The contribution of the three heat transfer resistances to the spreading of the advancing temperature front
- The thermal efficiency of one-pass operations
- The thermal efficiency of periodic cocurrent operations
- The thermal efficiency of periodic countercurrent operations

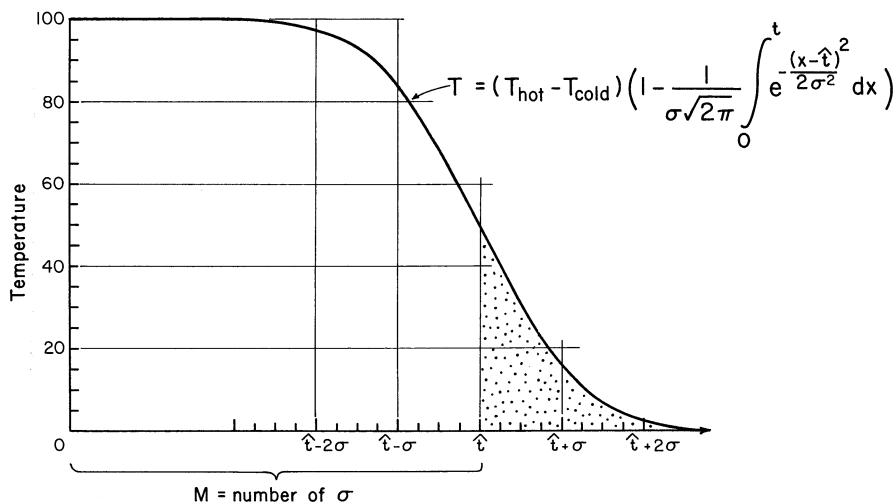


Fig. 15.8 Shape of the advancing hot temperature front, according to the dispersion model

15.3.1 Evaluation of σ^2 , the Quantity Which Represents the Spreading of the Temperature Front

The dispersion (or diffusion type) model leads to a symmetrical S-shaped advancing temperature front which represents the integral of the Gaussian distribution function. This S-shaped curve is characterized completely by a single quantity, the variance σ^2 . Figure 15.8 shows how the temperature front spreads with σ .

From diffusion theory, if the individual contributions to the spreading act independently, then one can add variances for the individual contributions or

$$\left(\begin{array}{c} \text{Spreading of} \\ \text{temperature} \\ \text{front} \end{array} \right)^2 = \left(\begin{array}{c} \text{spreading caused} \\ \text{by deviation from} \\ \text{plug flow} \end{array} \right)^2 + \left(\begin{array}{c} \text{spreading caused} \\ \text{by surface heat} \\ \text{transfer resistance} \end{array} \right)^2 \\ + \left(\begin{array}{c} \text{spreading caused} \\ \text{by resistance to} \\ \text{conduction in solid} \end{array} \right)^2$$

or in symbols

$$\sigma^2 = \sigma_{\text{axial gas dispersion}}^2 + \sigma_{\text{film resistance}}^2 + \sigma_{\text{particle heating}}^2 \quad (15.12)$$

If it is assumed in addition that no heat travels along the solids in the direction of gas flow (reasonable for a packed bed of spherical or randomly packed nonmetallic particles, but possibly not reasonable for a compact exchanger or monolith structure), then Levenspiel (1984), using the results of Sagara et al. (1970), has shown that equation (15.12) becomes, term for term,

$$M^2 = \frac{\sigma^2}{\hat{t}^2} = \frac{6L_p}{L} + \frac{2G_0C_g}{haL} + \frac{6G_0C_gL_p}{5k_saL} \quad (15.13)$$

where

$$L_p = \frac{\text{volume of particle}}{\text{surface of particle}}, \text{ characteristic length of particle [m]}$$

$$= \frac{R}{3} \text{ for spherical particle}$$

$$= \frac{R}{2} \text{ for cylindrical particle}$$

$$a = \frac{\text{exterior surface of particles}}{\text{volume of regenerator}}, \text{ specific surface [m}^{-1}\text{]}$$

$$= \frac{3(1-\epsilon)}{R} \text{ for spherical particles}$$

$$k_s, k_g = \text{thermal conductivity of solid and gas [W/mK]}$$

$$C_s, C_g = \text{specific heat of gas and solid [J/kgK]}$$

$$G_0 = u_0\rho, \text{ superficial mass velocity of gas [kg/m}^2\text{ s]}$$

$$M = \text{measure of the spreading temperature front in the vessel, see equations (15.12) and (15.13)}$$

For spherical particles equation (15.13) becomes

$$M^2 = \frac{\sigma^2}{\hat{t}^2} = \frac{d_p}{L} + \frac{1}{3(1-\epsilon)} \cdot \frac{G_0C_gd_p}{hL} + \frac{1}{30(1-\epsilon)} \cdot \frac{G_0C_gd_p^2}{k_sL} \quad (15.14)$$

This expression shows that as the exchanger is made longer, the relative spread of the temperature front becomes smaller; hence, the efficiency of the unit more closely approaches the flat front ideal.

Let us now see how to evaluate the thermal efficiency for various operating patterns knowing the value of σ^2 from equation (15.13) or (15.14).

15.3.2 One-Pass Operations; Dispersion Model

Consider a step input of hot fluid into a cold regenerator. After time \hat{t} the temperature distribution of solids in the regenerator will be as shown in Fig. 15.9.

The efficiency of heat capture by the solids after time \hat{t} can be found by referring to Fig. 15.9. Thus,

$$\eta_{\text{single pass}} = \left(\frac{\text{fractional heat recovery}}{\text{hatched area in Fig. 15.9}} \right) = 1 - \frac{\text{dotted area in Fig. 15.9}}{\text{area } ABCD} \tag{15.15}$$

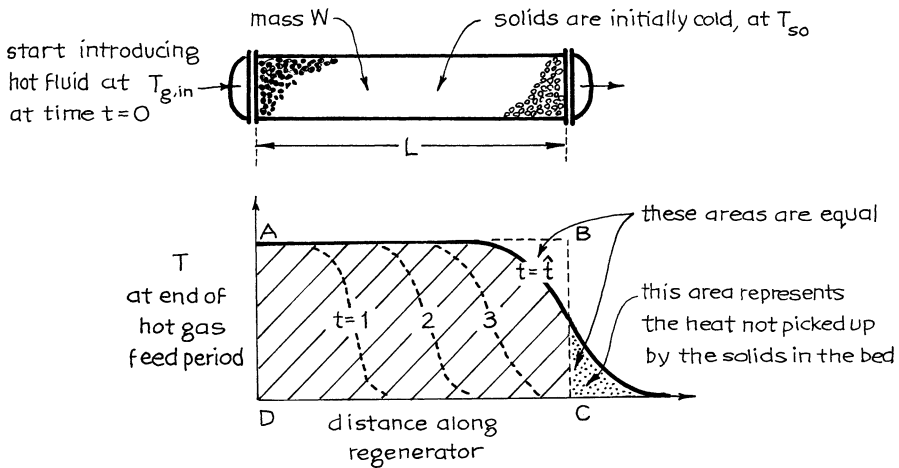


Fig. 15.9 Temperature of solids in a regenerator in a one-pass operation, according to the dispersion model

Noting that the S-shaped curve of Fig. 15.9 represents the Gaussian integral shown in Fig. 15.8 and that the dotted area is calculated to be 0.4σ , the single-pass efficiency is then

$$\eta = 1 - \frac{0.4\sigma M}{\sigma} = 1 - 0.4M \quad \text{for } M \leq 0.4 \tag{15.16}$$

The upper line of Fig. 15.10 then shows how the single-pass efficiency depends on the value of M .

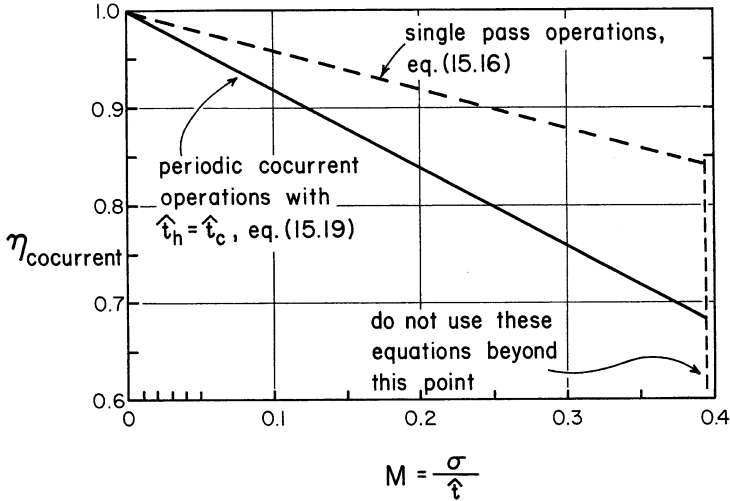


Fig. 15.10 Periodic cocurrent operations always lead to a lower efficiency than do single-pass operations. Both curves are drawn for a switching time of \hat{t} and are based on the dispersion model

Note that the condition $M \leq 0.4$ is attached to equation (15.16). This represents operations where the solids at the inlet do reach the temperature of the hot incoming gas. This is what we call a *long regenerator*. When $M > 0.4$ the temperature profile of Fig. 15.9 is so broad that the solids at the inlet do not reach $T_{g, \text{in}}$ and the efficiency deviates from equation (15.16). We call this a *short regenerator*. From now on we only consider long regenerators.

The efficiency for an operating time \hat{t} is of interest because in periodic operations a value of switching time $t_{sw} = \hat{t}$ normally is optimum in that it gives highest efficiency of heat recovery.

15.3.3 Periodic Cocurrent Operations with Equal Flow Rates of Hot and Cold Fluids or $\hat{t}_h = \hat{t}_c = t_{sw}$ Dispersion Model

Suppose we choose to switch from hot to cold fluid at time \hat{t} and back again after an additional time \hat{t} . The temperature distribution will then be somewhat as shown in Fig. 15.11, and reflection shows that the inefficiency in heat absorption during heating is represented by the shaded areas A and B. Thus, the efficiency is given by

$$\eta_{\text{heating}} = 1 - \left(\frac{\text{area A} + \text{area B}}{\text{area WXYZ}} \right) \text{ Fig. 15.11}$$

From equations (15.15) and (15.16) this becomes

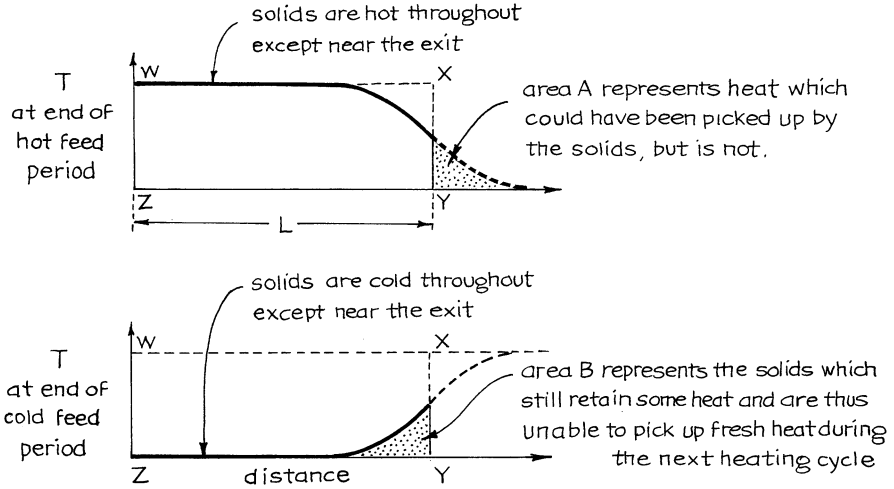


Fig. 15.11 Temperature of solids for symmetric periodic cocurrent flow with $\hat{t}_h = \hat{t}_c = t_{sw}$, according to the dispersion model

$$\eta_{\text{heating}} = 1 - 0.8M \tag{15.17}$$

and for these symmetric operations

$$\eta_{\text{cooling}} = \eta_{\text{heating}} \tag{15.18}$$

An analysis of the situation leads to the following conclusions:

1. The highest efficiency always occurs when the switching time t_{sw} is chosen to be \hat{t} .
2. Whenever $M \leq 0.4$ the succeeding temperature fronts of Fig. 15.11 do not affect each other. Thus, the previous front is swept out before the next one comes along. In this situation reflection shows that the efficiency is given by

$$\eta_{\text{periodic cocurrent}} = 2\eta_{\text{single pass}} - 1 \tag{15.19}$$

3. Figure 15.10 shows how the efficiency of single-pass and periodic cocurrent operations depends on the value of M .

15.3.4 Periodic Countercurrent Operations with Equal Flow Rates of Hot and Cold Fluids or $\hat{t}_h = \hat{t}_c$ Dispersion Model

Starting with hot fluid entering a cold regenerator, successive temperature fronts will look somewhat as shown in Fig. 15.12.

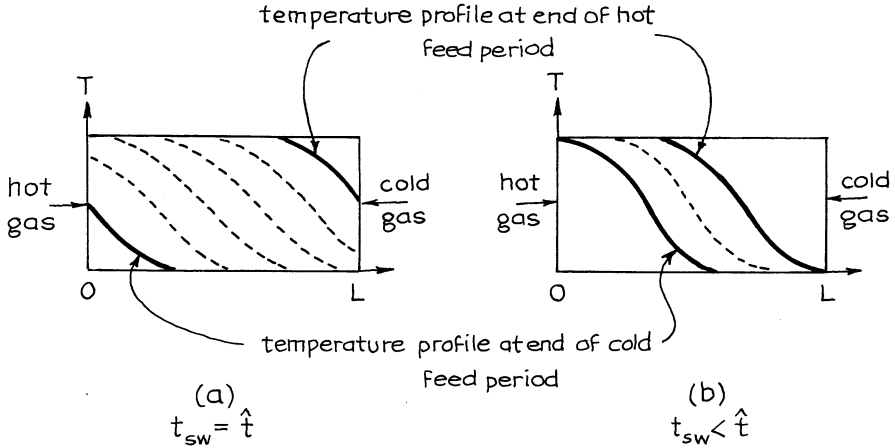


Fig. 15.12 Temperature shifts in solids for symmetric counterflow, thus for $\hat{t}_h = \hat{t}_c$, according to the dispersion model

As the temperature profile shifts back and forth, from right to left, dispersion will make the front spread. However, in partially heating a cold particle, it is the outside shell which heats first, and it is this which first cools with cold gas. This results in a self-healing of the spreading front or a tendency to approach a flat front profile.

The overall effect of these two opposing effects is something which cannot be evaluated by the analyses of today. Probably the best compromise at this time, and until we know better, is to assume that the temperature front remains unchanged from the one pass to the next. We use this assumption throughout for the counter-current operations.

Again, noting that the temperature profiles follow the integral of the Gaussian distribution, the thermal efficiency is evaluated with the aid of Fig. 15.13 and the following calculation procedure:

- (a) Determine $\hat{t}_h = \hat{t}_c = \hat{t}$ from equations (15.5) and (15.6).
- (b) Set $t_{sw} \leq \hat{t}$.
- (c) Determine $\sigma_h = \sigma_c = \sigma$ from equation (15.13) or (15.14).
- (d) Calculate $\sigma_{sw} = \sigma(t_{sw}/\hat{t})^{1/2}$.
- (e) Calculate $P = (\hat{t} - t_{sw})/2\sigma_{sw}$.
- (f) Calculate $Q = t_{sw}/\sigma_{sw}$.

The efficiency is then given by

$$\eta = 1 - \left(\frac{\text{area } E \text{ and area } F}{\text{area } WXYZ} \right) \tag{15.20}$$

Fig. 15.13

This is a function of P and Q , as displayed in Fig. 15.14.

Note that if one can make t_{sw} smaller than $\hat{t} - 5\sigma_{sw}$, then one can get almost complete heat recovery, as long as the temperature profile stays balanced between

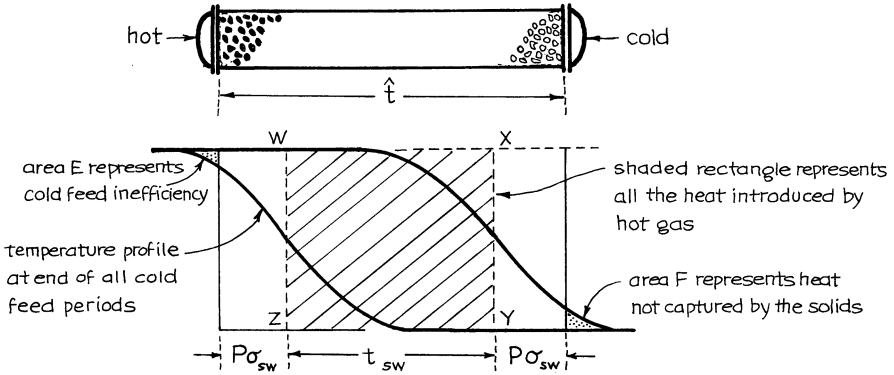


Fig. 15.13 Graph which shows how the efficiency of heat recovery is determined for symmetric counterflow, thus for $\hat{t}_h = \hat{t}_c$

the two ends of the regenerator. However, as t_{sw} is allowed to approach \hat{t} , the efficiency drops to that of one-pass operations, and for $t_{sw} > \hat{t}$ the efficiency drops rapidly toward zero.

Comparing Fig. 15.14 with Fig. 15.10 shows that symmetric countercurrent operations can be much more efficient than symmetric cocurrent operations; just use a shorter switching time.

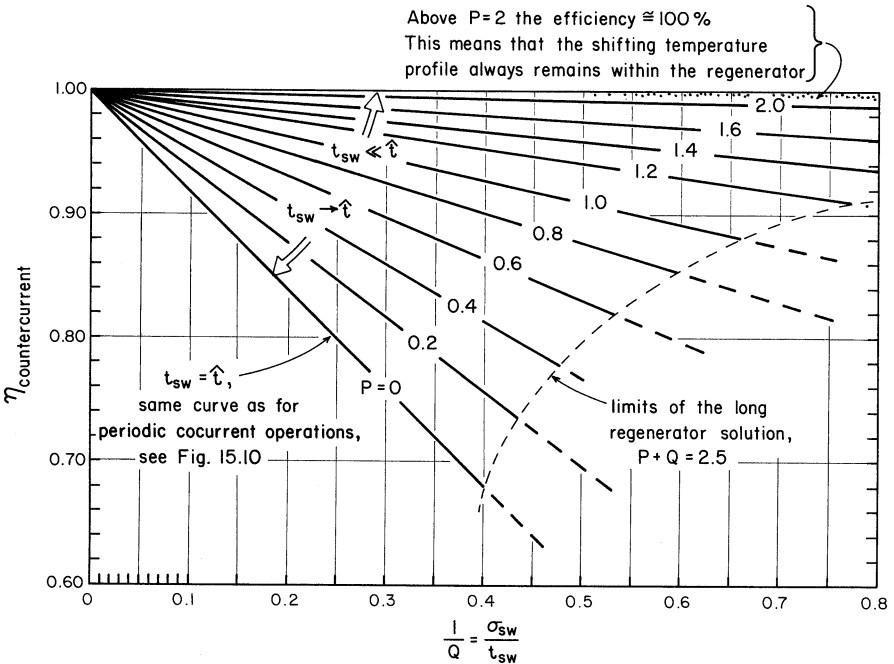


Fig. 15.14 Efficiency of symmetric counterflow, thus for $\hat{t}_h = \hat{t}_c$

15.3.5 Comments on the Dispersion Model

1. Countercurrent operations always give higher efficiencies than do cocurrent operations.
2. No matter what contacting scheme is used, the longer the exchanger, the higher will be its efficiency, with a limiting value given by the flat front model.
3. For short exchangers ($\sigma > 0.4 \hat{t}$ or $\sigma > 0.4 t_{sw}$) the assumptions of the dispersion model do not represent reality too well, the efficiency predictions of the model become too high, and thus, the model should not be used for anything but as a crude approximation.
4. The analysis of this section only applies to exchangers having negligible heat conduction through the solids in the direction of gas flow. Thus, it applies reasonably to packed bed regenerators and to monolith regenerators made of ceramic or other poorly conducting solids.

For metallic monoliths where conduction along the metal is significant, the efficiencies calculated in this chapter should be lowered somewhat, to give behavior somewhere between the packed bed and the fluidized bed (see next section).

5. For dusty gases countercurrent operations have an additional advantage in that they help avoid plugging of the regenerator.
6. For the rotating-wheel regenerator the value of the switching time is related to the time that a section of the wheel spends in the cold gas and in the hot gas. Thus, the time for one rotation of the wheel should be $2 t_{sw}$.
7. For a given flow rate of hot and cold gases through a rotating regenerator, changing the fraction of wheel seeing hot gas and seeing cold gas (see Fig. 15.15) does not affect operations substantially because although this changes $t_{sw, h}$ and $t_{sw, c}$, it also changes \hat{t}_h and \hat{t}_c in the same proportion. Hence, it is recommended that 50 % of the wheel see one fluid and 50 % the other.

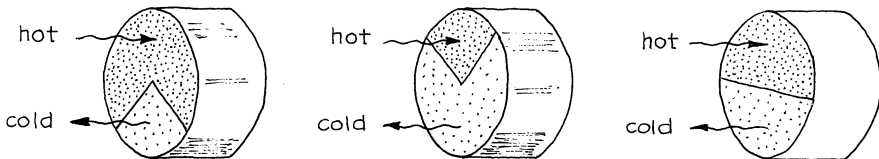


Fig. 15.15 Various geometries for the rotating-wheel regenerator

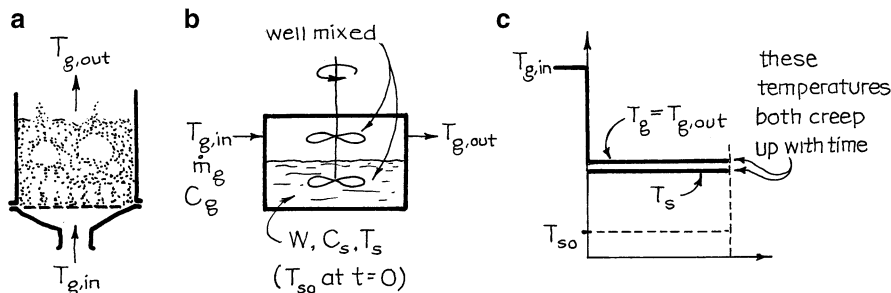


Fig. 15.16 The heating of a batch of solids in a fluidized bed regenerator, (a) sketch of unit, (b) contacting model, and (c) temperatures in the unit

15.4 Fluidized Bed Regenerators

Fluidized beds of fine particles are characterized by good mixing of solids and $Ua \rightarrow \infty$ (see Chap. 14). Thus, we may take the solids to be uniform in temperature at any time and the leaving gas to be at the temperature of the solids, as sketched in Fig. 15.16. A heat balance around the whole vessel becomes

$$\dot{m}_g C_g (T_{g, \text{in}} - T_s) = W_s C_s \frac{dT_s}{dt} \quad (15.21)$$

Separating and integrating then give

$$\frac{T_{g, \text{in}} - T_s}{T_{g, \text{in}} - T_{s0}} = \frac{\Delta T}{\Delta T_0} = e^{-t/\hat{t}} \quad \text{where } \hat{t} = \frac{W_s C_s}{\dot{m}_g C_g} \quad (15.22)$$

Graphically this temperature progression is shown in Fig. 15.17. Note that equation (15.22) is a special case of the corresponding recuperator expression, equation (13.24), in which $Ua \rightarrow \infty$.

Let us consider the thermal efficiency of fluidized bed recuperators.

15.4.1 Efficiency of One-Pass Operations

Suppose cold gas enters a hot fluidized bed. At the start the gas leaves hot and the efficiency is 100%. But with time the temperature of solids and exit gas will decrease as shown in Fig. 15.17 and the point efficiency of operations will likewise decrease. Referring to Fig. 15.18 the average efficiency for an operating period t_{sw} is then

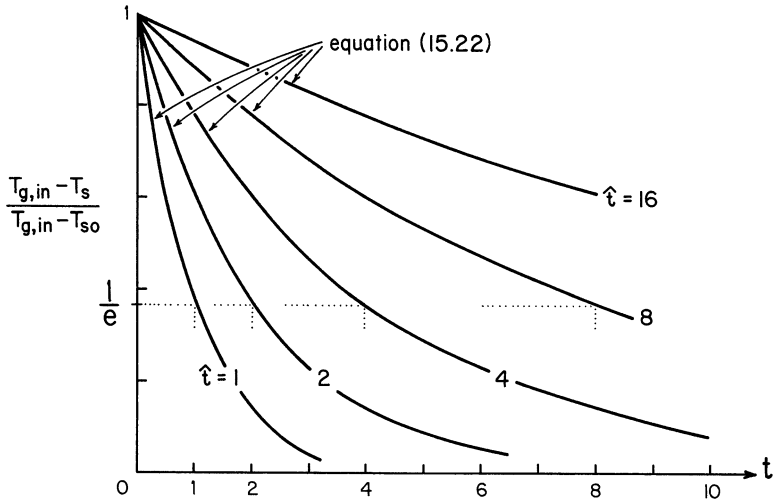


Fig. 15.17 Temperature–time curves when a batch of hot fluidized solids is cooled by a cold gas stream

$$\bar{\eta} = \frac{\text{dotted area in Fig. 15.20}}{\text{area } ABCD} = \frac{\int_0^{t_{sw}} e^{-t/\hat{t}} dt}{t_{sw}} \tag{15.23}$$

Performing the integration gives

$$\bar{\eta} = \frac{\hat{t}}{t_{sw}} \left(1 - e^{-t_{sw}/\hat{t}} \right) \tag{15.24}$$

Figure 15.19 shows that the efficiency starts at 100 % at the beginning of the run and then slides to zero; thus, the shorter the operating time, the more efficient is the regenerator for one-pass operations.

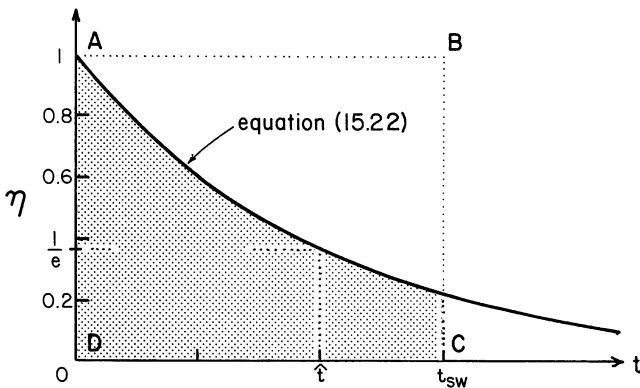


Fig. 15.18 Efficiency of heat recovery at different times during a one-pass operation of a fluidized bed regenerator

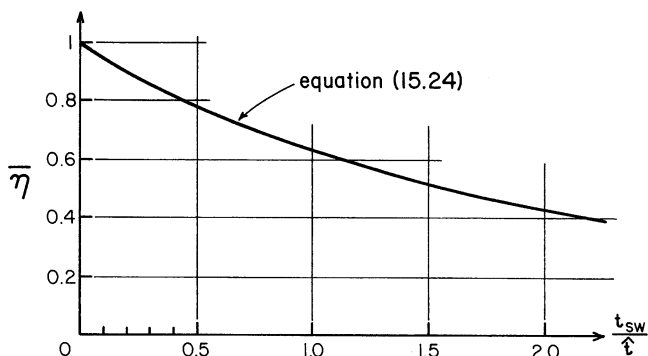


Fig. 15.19 Average heat recovery efficiency in a one-pass operation of a fluidized bed regenerator

15.4.2 Efficiency of Periodic Operations

First, consider the situation where $\hat{t}_h = \hat{t}_c$. Here the temperature of the fluidized bed regenerator varies with time as shown in Fig. 15.20, and for optimum operations with given t_{sw} , symmetry suggests that we should keep

$$1 - y_2 = y_1, \text{ in Fig. 15.20}$$

The efficiency of operations is then obtained from integration of equation (15.23), using the limits t_1 and t_2 . This gives

$$\bar{\eta} = \frac{\hat{t}}{t_{sw}} (y_1 - y_2)$$

where

$$y_1 = e^{-t_1/\hat{t}}, \quad y_2 = e^{-t_2/\hat{t}}, \quad \text{and} \quad t_{sw} = t_2 - t_1$$

Combining the above five expressions, eliminating y_1, y_2, t_1, t_2 , and simplifying then give

$$\bar{\eta} = \frac{\hat{t}}{t_{sw}} \left(\frac{e^{t_{sw}/\hat{t}} - 1}{e^{t_{sw}/\hat{t}} + 1} \right) \tag{15.25}$$

From the geometry of Fig. 15.20, we can see that when the switching time approaches zero, the efficiency reaches a maximum of 50 %, and as the switching time is increased, the efficiency decreases toward zero.

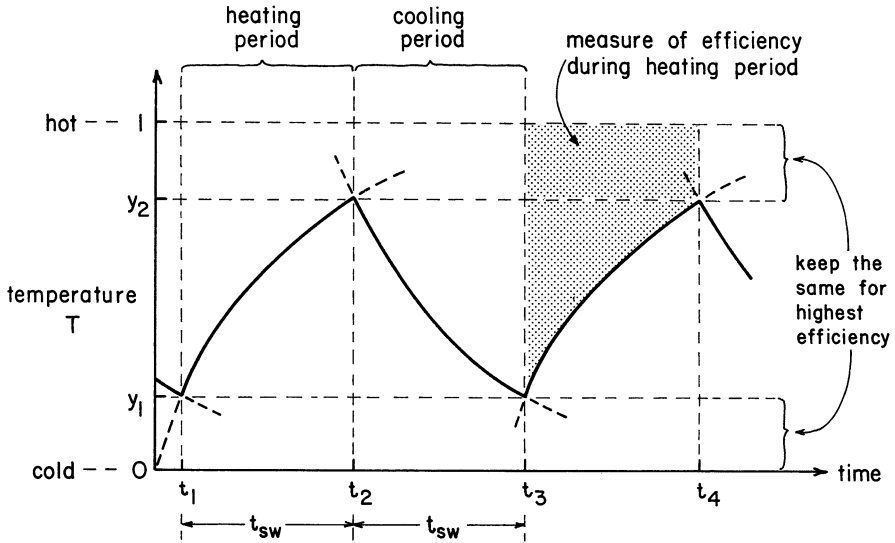


Fig. 15.20 Temperature changes for symmetric period operations ($\hat{t}_h = \hat{t}_c$) of a fluidized bed regenerator

15.4.3 Comments on Fluidized Bed Regenerators

The analysis of this section leads to the following conclusions:

1. Single-stage periodic operation with $\hat{t}_h = \hat{t}_c$ has efficiencies approaching a maximum of 50 % for very frequent switching times. For longer switching times the efficiency drops toward zero.
2. Efficiencies for single-stage fluidized bed operations are very much lower than for packed bed operations; hence, these units are not used in practice.
3. Multistage fluidized bed operations will give higher efficiencies than single-stage operations. However, the large power requirement needed to fluidize the large mass of solids and the still lower efficiency when compared to a well-designed packed bed regenerator are reasons for not using such units in practice.

Example 15.1 The Great Paperweight Disaster

Idiot!! Can't you read!! The order said, "One vermillion paperweight," not one million paperweights. And here we've already made 999,239 of these beauties. What will we do with the extra 999,238 that we have in our storehouse? You'd better come up with an answer quick or else you lose your job and the West Coast Paperweight Co. goes out of business.

One possibility is to sell them as packing ($\varepsilon = 0.4$) for a pair of unique, deluxe extra-high-efficiency heat regenerators, each 1 m^2 in cross section.

(continued)

Example 15.1 (continued)

Hot and cold gases would then be passed successively through these units at a superficial gas velocity of 4 m/s measured at 20 °C and 1 atm.

- For cocurrent operations find the desired switching time $t_{sw} = \hat{t}$ and the efficiency of operations.
- For counterflow operations find the efficiency of operations for a switching time $t_{sw} = \hat{t}$.
- For counterflow operations find the efficiency of operations for a switching time $t_{sw} = 0.75 \hat{t}$.

Data: For the nearly spherical crown glass paperweights,

$$d_p = 0.05 \text{ m}$$

$$\phi = 0.94, \text{ sphericity}$$

$$k_s = 1.066 \text{ W/m K}$$

$$C_s = 714 \text{ J/kg K}$$

$$\rho_s = 2,500 \text{ kg/m}^3$$

Take equal quantities of hot and cold gases, and to keep things simple, assume that they have the same properties as air at 20 °C. From the appendix we find these properties to be

$$\mu = 1.8 \times 10^{-5} \text{ kg/m s}$$

$$C_g = 1,013 \text{ J/kg K}$$

$$\rho_g = 1.2 \text{ kg/m}^3$$

$$k_g = 0.026 \text{ W/m K}$$

$$(mw) = 0.0289 \text{ kg/mol}$$

Solution

We will solve this problem with the dispersion model, but first some preliminaries.

- Height of paperweight-filled regenerators:

$$L = \left(\frac{999,238 pw}{2} \right) \left[\frac{\pi (0.05)^3 \text{ m}^3 \text{ solid}}{pw} \right] \left(\frac{1 \text{ m}^3 \text{ reg}}{0.6 \text{ m}^3 \text{ solid}} \right) \left(\frac{1}{1 \text{ m}^2 \text{ c.s.}} \right) = 54.5 \text{ m each}$$

(continued)

2. Mass flow rate and superficial mass velocity of gas:

$$\dot{m} = \left(4 \frac{m}{s}\right) \left(\frac{1 \text{ m}^3 \text{ vol}}{1 \text{ m height}}\right) \left(\frac{1 \text{ mol}}{0.0224 \text{ m}^3}\right) \left(\frac{0.0289 \text{ kg}}{\text{mol}}\right) \left(\frac{273}{293}\right) = 4.8 \text{ kg/s}$$

and

$$G_0 = \frac{\dot{m}}{A} = 4.8 \text{ kg/m}^2 \text{ s}$$

3. Heat transfer coefficient between gas and pw packing is given by equation (9.37). Evaluating the needed dimensionless groups gives

$$\text{Re}_p = \frac{d_p u_0 \rho_g}{\mu} = \frac{(0.05)(4)(1.2)}{1.8 \times 10^{-5}} = 13,333$$

$$\text{Pr} = \frac{C_g \mu}{k_g} = \frac{(1,013)(1.8 \times 10^{-5})}{(0.026)} = 0.7013$$

Thus, equation (9.37) becomes

$$\frac{h(0.05)}{0.026} = 2 + 1.8(13,333)^{1/2}(0.7013)^{1/3}$$

giving

$$h = 97.06 \text{ W/m}^2 \text{ K}$$

4. Calculate \hat{t} , the time needed to cool or to heat the solids. From equation (15.5),

$$\hat{t} = \frac{W_s C_s}{\dot{m}_g C_g} = \frac{[(54.5)(2,500)(0.6)](714)}{(4.80)(1,013)} = 12,000 \text{ s}$$

$$= 2 \text{ h } 20 \text{ min}$$

5. Calculate the spreading of the temperature front. From equation (15.14),

$$M^2 = \frac{\sigma^2}{\hat{t}^2} = \frac{d_p}{L} + \frac{1}{3(1-\varepsilon)} \cdot \frac{G_0 C_g d_p}{hL} + \frac{1}{30(1-\varepsilon)} \cdot \frac{G_0 C_g d_p^2}{k_s L}$$

Replacing all values gives

(continued)

$$M^2 = 0.0009 + 0.0255 + 0.0116 = 0.0381$$

or

$$M = \frac{\sigma}{\hat{t}} = 0.1952$$

6. Single-pass efficiency. From equation (15.16) or Fig. 15.10,

$$\eta_{\text{single pass}} = 1 - 0.4(0.1952) = 0.9219, \text{ or } 92\%$$

We are now ready to solve the problem.

(a) Cocurrent flow with $t_{sw} = \hat{t}$. From equation (15.19) or Fig. 15.10,

$$\eta_{\text{cocurrent}} = 2(0.9219) - 1 = 0.8438, \text{ or } 84\%$$

(b) Counterflow with $t_{sw} = \hat{t}$. From the procedure leading to Fig. 15.14,

$$\sigma_h = \sigma_c = \sigma_{sw} = M\hat{t} = 0.1952(12,000) = 2,342 \text{ s}$$

$$P = \frac{\hat{t} - t_{sw}}{2\sigma_{sw}} = 0$$

$$\frac{1}{Q} = \frac{\sigma_{sw}}{t_{sw}} = \frac{2,343}{12,000} = 0.1952$$

Then, from Fig. 15.14

$$\eta_{\text{counter}} = 0.8438, \text{ or } 84\% \quad (\text{same as for single pass})$$

(c) Counterflow with $t_{sw} = 0.75\hat{t} = 0.75(12,000) = 9,000 \text{ s}$. Following the procedure of Section III.D, we have

$$\sigma_h = \sigma_c = (0.1952)(12,000) = 2,342 \text{ s}$$

$$\sigma_{sw} = 2,342 \left(\frac{9,000}{12,000} \right)^{1/2} = 2,028 \text{ s}$$

$$P = \frac{12,000 - 9,000}{2(2,028)} = 0.7396$$

$$\frac{1}{Q} = \frac{2,028}{9,000} = 0.2253$$

Then, from Fig. 15.13

$$\eta_{\text{counter}} \cong 94\%$$

Note that counterflow with a smaller switching time gives a higher exchange efficiency.

Problems on Regenerators

- 15.1. The geometry for the regenerator of example 15.1 is not satisfactory because it is too tall and skinny. If we made the regenerator one-quarter the height and double the diameter but maintained the same volumetric flow rate of gases, what would be the cocurrent and counterflow efficiencies of this modified design for the cases of example 15.1?
- 15.2. We want four times the flow rate of gases of example 15.1. For this we plan to double the diameter and reduce the height of the regenerator of example 15.1, but keep u_0 unchanged at 4 m/s. What would be the cocurrent and counterflow efficiencies of this operation for the cases of example 15.1?
- 15.3. Two packed bed regenerators are used in periodic swing operations to recover heat from hot exchange gases at 800 °C and to preheat inlet air at 100 °C. Each generator is 30 m long and 4-m diameter. Solid pebbles used are approximately spherical and 6-cm diameter. Find the heat recovery efficiency:
- For cocurrent operations at the optimum switching time. Use the dispersion model.
 - For cocurrent operations at the optimum switching time. Use the flat front model.
 - For cocurrent operations with a 7.2-h switching time. Use the flat front model.
 - For cocurrent operations with an 18-h switching time. Use the flat front model.

<i>Data : Solids</i>	<i>Mean gas properties, at 450 °C</i>
$\rho_s = 3,900 \text{ kg/m}^3$	$\mu = 3 \times 10^{-5} \text{ kg/m} \cdot \text{s}$
$C_s = 1,000 \text{ J/kg K}$	$C_g = 1,020 \text{ J/kg K}$
$k_s = 0.5 \text{ W/m} \cdot \text{k}$	$k_g = 0.05 \text{ W/m} \cdot \text{k}$
$\varepsilon = 0.4$	$\rho = 0.5 \text{ kg/m}^3$
$d_p = 6 \text{ cm}$	Use $t_{sw, c} = t_{sw, h}$ throughout

Note. This problem is related to that treated by Dudukovic and Ramachandran, *Chem. Eng.*, pg. 70 (June 10, 1985).

- 15.4. Repeat the previous problem with the change of using countercurrent flow instead of cocurrent flow. Find the heat recovery efficiency.
- For $t_{sw} = \hat{t}_h = \hat{t}_c$, using the dispersion and then the flat front models.

(b) For a switching time $t_{sw} = 7.2$ h, again using the dispersion model and then the flat front model.

15.5. The laboratory's high-temperature wind tunnel experiment requires an air-flow of 30 m/s at 540 °C and 1 atm through a square test section of 0.3 m \times 0.3 m. One way to do this is to take in ambient air at 20 °C and heat it continually.

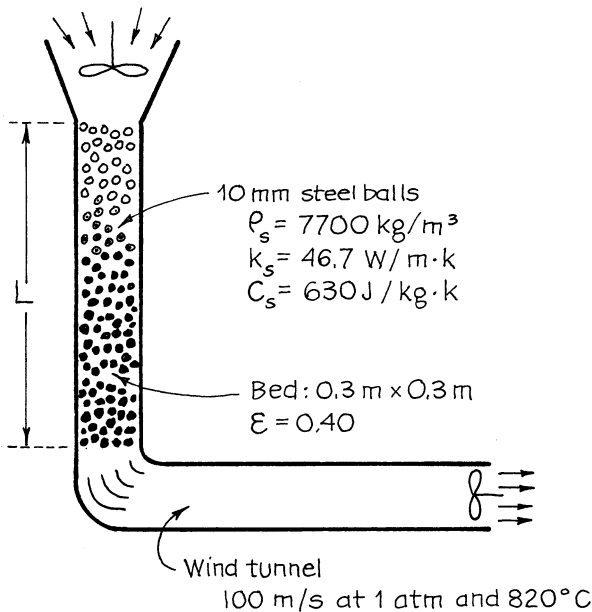
(a) Find how many household electric heaters, rated at 1,500 W, would be needed to provide this hot air continually during the run.

Alternatively, we can leisurely heat up a packed bed of rocks or other solid beforehand as shown below, and at the start of the run, blow through the required ambient air at 20 °C, this representing a one-pass operation.

(b) What length of packed bed and how many tons of steel balls would be required to store the heat needed for a 15-min wind tunnel experiment? Assume the flat front approximation for this calculation.

(c) How long can we run a hot-air wind tunnel experiment with the stored heat from an 8-m-high bed of steel balls? Note that at 2.5σ away from the mean, the S-shaped dispersion curve is within 1 % of its asymptote.

Data: Take 300 °C to be the average conditions of air in the packed bed; see diagram for additional data.



- 15.6. Repeat Problem 15.5, but instead of using steel balls in the regenerator, let us use uniformly sized crushed rock from the local rock quarry.

Data: For rock,

$$d_p = 0.05 \text{ m} \quad k_s = 0.80 \text{ W/kg K}$$

$$\rho_s = 2,190 \text{ kg/m}^3 \quad \varepsilon = 0.48$$

$$C_s = 800 \text{ J/kg K}$$

- 15.7. A pair of regenerators 32 m high and 3 m in diameter filled with uniformly sized and close to spherical basaltic beach stones is to be used to transfer heat from hot waste gases leaving a process to cold incoming air. For equal flows of hot and cold gases and for the following operating conditions and properties of materials, find:

- The relative contributions of the three resistances to heat transfer
- The switching time to use and the efficiency of heat recovery for the best cocurrent operations
- The efficiency of heat recovery for countercurrent operations with a switching time $t_{sw} = 2 \text{ h}$

Data: For the solid,

$$d_p = 0.08 \text{ m} \quad k_s = 0.5 \text{ W/m K}$$

$$\rho_s = 2,280 \text{ kg/m}^3 \quad C_s = 1,000 \text{ J/kg K}$$

In the regenerator

$$\varepsilon = 0.4$$

$$G_0 = 3.6 \text{ kg/m}^2 \text{ s (or } u_0 \cong 3 \text{ m/s at } 20^\circ \text{C).}$$

For both hot and cold gases, take the properties of air at 20°C and 1 atm; see example 15.1.

A rotating-wheel regenerator is to transfer heat from hot combustion gases [6,000 mol/min, $1,000^\circ \text{C}$, $C_p = 30 \text{ J/mol K}$, $(mw) = 0.03 \text{ kg}$] to cold incoming air [6,000 mol/min, 0°C , $C_p = 30 \text{ J/mol K}$, $(mw) = 0.03 \text{ kg}$]. The wheel is to be 1 m in diameter and 0.73 m thick and is to consist of a tortuous path stainless steel honeycomb ($\rho_s = 7,700 \text{ kg/m}^3$, $C_s = 500 \text{ J/kg K}$, $\varepsilon = 0.8$). For maximum efficiency, what should be the rate of rotation of the wheel, and what can we expect the outlet gas temperatures to be?

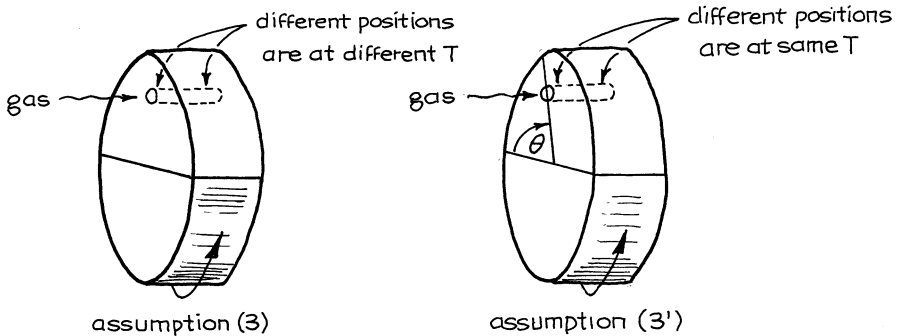
- 15.8. As a first approximation:

- Assume no heat flow resistance from gas to metal (or $h \rightarrow \infty$) and into the metal sheet.
- Assume plug flow of gas through the regenerator.

- (3) Assume that the regenerator is so built that no heat flows from one location in the metal to another.

15.9. Replace assumption (3) with the following:

- (3') Assume that there is no resistance to heat flow in the metal along a flow channel; thus, all the metal at a given angle θ in the drawing below is at the same temperature.



15.10. A pair of identical fluidized beds is to be used to recover heat from hot waste gas leaving a process and transfer it to fresh incoming gas. What thermal recovery efficiency may be expected from this pair of regenerators if the switching time is set at:

- (a) 15 min?
(b) 30 min?

Data: Weight of sand in each regenerator = 570 kg. For both hot and cold gases, take the properties of air at 20 °C. Flow rate of hot and cold gases = 0.5 kg/s.

References

- H. Hausen, *Heat Transfer in Counterflow, Parallel-Flow, and Cross-Flow* (trans. from German by M.S. Sayer), (McGraw-Hill, New York, 1983)
 M. Jakob, *Heat Transfer*, vol. 2, Chapter 35, (Wiley, New York, 1957)
 D.Q. Kern, *Process Heat Transfer* (McGraw-Hill, New York, 1950)

- O. Levenspiel, Design of long heat regenerators by use of the dispersion model, *Chem. Eng. Sci.* **38**[12], 2035–2045 (1983)
- W.H. McAdams, *Heat Transmission*, 3rd edn. (McGraw-Hill, New York, 1954)
- M. Sagara, P. Schneider, J.M. Smith, The determination of heat-transfer parameters for flow in packed beds using pulse testing and chromatographic theory. *Chem. Eng. J.* **1**, 47 (1970)